A Novel Subfamily Endo-β-1,4-glucanase in Glycoside Hydrolase Family 10

Article *in* Applied and Environmental Microbiology · June 2019

DOI: 10.1128/AEM.01029-19

9 authors, including:

Yi Zhang
Tianjin University
118 PUBLICATIONS **1,665** CITATIONS
SEE PROFILE

Chun-Yang Li
Shandong University
44 PUBLICATIONS **487** CITATIONS
SEE PROFILE

Ping Wang
Washington University in St. Louis
508 PUBLICATIONS **10,834** CITATIONS
SEE PROFILE

Xiu-Lan Chen
Shandong University
286 PUBLICATIONS **4,957** CITATIONS
SEE PROFILE

AMERICAN SOCIETY FOR MICROBIOLOGY | Applied and Environmental Microbiology®

ENZYMOLOGY AND PROTEIN ENGINEERING

A Novel Subfamily of Endo-β-1,4-Glucanases in Glycoside Hydrolase Family 10

Fang Zhao,[a] Hai-Yan Cao,[a] Long-Sheng Zhao,[a] Yi Zhang,[a] Chun-Yang Li,[a,b] Yu-Zhong Zhang,[a,b,c] Ping-Yi Li,[a] Peng Wang,[a] Xiu-Lan Chen[a]

[a]State Key Laboratory of Microbial Technology, Institute of Marine Science and Technology, Marine Biotechnology Research Center, Shandong University, Qingdao, China

[b]College of Marine Life Sciences, Institute for Advanced Ocean Study, Ocean University of China, Qingdao, China

[c]Laboratory for Marine Biology and Biotechnology, Qingdao National Laboratory for Marine Science and Technology, Qingdao, China

ABSTRACT As classified by the Carbohydrate-Active Enzymes (CAZy) database, enzymes in glycoside hydrolase (GH) family 10 (GH10) are all monospecific or bifunctional xylanases (except a tomatinase), and no endo-β-1,4-glucanase has been reported in the family. Here, we identified *Arcticibacterium luteifluviistationis* carboxymethyl cellulase (*Al*CMCase) as a GH10 endo-β-1,4-glucanase. *Al*CMCase originated from an Arctic marine bacterium, *Arcticibacterium luteifluviistationis* SM1504^T. It shows low identity (<35%) with other GH10 xylanases. The gene encoding *Al*CMCase was overexpressed in *Escherichia coli*. Biochemical characterization showed that recombinant *Al*CMCase is a cold-adapted and salt-tolerant enzyme. *Al*CMCase hydrolyzes cello- and xylo-configured substrates via an endoaction mode. However, in comparison to its significant cellulase activity, the xylanase activity of *Al*CMCase is negligible. Correspondingly, *Al*CMCase has remarkable binding capacity for cello-oligosaccharides but no obvious binding capacity for xylo-oligosaccharides. *Al*CMCase and its homologs are grouped into a branch separate from other GH10 xylanases in a phylogenetic tree, and two homologs also displayed the same substrate specificity as *Al*CMCase. These results suggest that *Al*CMCase and its homologs form a novel subfamily of GH10 enzymes that have robust endo-β-1,4-glucanase activity. In addition, given the cold-adapted and salt-tolerant characters of *Al*CMCase, it may be a candidate biocatalyst under certain industrial conditions, such as low temperature or high salinity.

IMPORTANCE Cellulase and xylanase have been widely used in the textile, pulp and paper, animal feed, and food-processing industries. Exploring novel cellulases and xylanases for biocatalysts continues to be a hot issue. Enzymes derived from the polar seas might have novel hydrolysis patterns, substrate specificities, or extremophilic properties that have great potential for both fundamental research and industrial applications. Here, we identified a novel cold-adapted and salt-tolerant endo-β-1,4-glucanase, *Al*CMCase, from an Arctic marine bacterium. It may be useful in certain industrial processes, such as under low temperature or high salinity. Moreover, *Al*CMCase is a bifunctional representative of glycoside hydrolase (GH) family 10 that preferentially hydrolyzes β-1,4-glucans. With its homologs, it represents a new subfamily in this family. Thus, this study sheds new light on the substrate specificity of GH10.

KEYWORDS Arctic seawater, cellulase, glycoside hydrolase family 10, novel subfamily, substrate specificity, xylanase

Cellulose and xylan, the two most abundant polysaccharides in nature, exist in the cell walls of terrestrial plants and a majority of marine algae (1). Cellulose consists of β-1,4-linked glucose. Its depolymerization depends on the cellulase synergies of endo-β-1,4-glucanases and exo-β-1,4-glucanases, and the released cello-oligosaccharides

Citation Zhao F, Cao H-Y, Zhao L-S, Zhang Y, Li C-Y, Zhang Y-Z, Li P-Y, Wang P, Chen X-L. 2019. A novel subfamily of endo-β-1,4-glucanases in glycoside hydrolase family 10. Appl Environ Microbiol 85:e01029-19. https://doi.org/10.1128/AEM.01029-19.

Editor Ning-Yi Zhou, Shanghai Jiao Tong University

Address correspondence to Peng Wang, wangwanlue@163.com, or Xiu-Lan Chen, cxl0423@sdu.edu.cn.

Received 5 May 2019
Accepted 26 June 2019
Accepted manuscript posted online 28 June 2019
Published 29 August 2019

and cellobiose are further hydrolyzed by β-glucosidases (2, 3). Xylan is a complex heteropolymer. Its 1,4-linked β-D-xylopyranosyl backbone can be replaced by α-L-arabinose, 4-*O*-methyl-glucuronic acid, acetate, or ferulic acid. The complete degradation of xylan requires a series of enzymes, including endo-β-1,4-xylanases, β-xylosidases, α-L-arabinofuranosidases, and carbohydrate esterases (4). Cellulase and xylanase are very important in the textile, pulp and paper, animal feed, and food-processing industries. Thus, exploring novel cellulases and xylanases continues to be a research highlight (2, 4).

Marine cellulase and xylanase play important roles in organic carbon degradation and cycling in the ocean. Under polar geochemical conditions, e.g., Arctic seawater, enzymes evolved to support the survival of microbes in these extreme environments (5, 6). These enzymes might present novel properties, such as cold adaptation, salt tolerance, or unique substrate specificity (7). Thus, marine-derived enzymes exhibiting these features have great potential for both fundamental research and industrial applications and deserve to be explored (4).

To date, 162 glycoside hydrolase (GH) families have been described in the Carbohydrate-Active Enzymes (CAZy) database and have been grouped into 18 GH clans (A to R) (8; http://www.cazy.org). The GH-A clan includes the families GH1, -2, -5, -10, -17, -26, -30, -35, -39, -42, -50, -51, -53, -59, -72, -79, -86, -113, -128, -147, -148, -157, and -158. Enzymes in the GH-A clan share similar $(\beta/\alpha)_8$ barrel (TIM-barrel) structures and adopt a retaining mechanism to act on substrates with two glutamate residues as the catalytic acid/base (9). GH10 enzymes reported so far include monospecific and bifunctional xylanases, which can attack the 1,4-linked β-D-xylopyranosyl backbone. Also, tomatinase activity has been reported in one case (10). Bifunctional enzymes in GH10 that mainly exhibit β-1,4-xylanase activity show additional β-1,3-xylanase (11), β-1,3-glucanase (12), or β-1,4-glucanase (13–16) activity. In comparison to their xylanase activity, GH10 bifunctional xylanases/cellulases display negligible cellulase activity (9, 13–16). Up to now, no endo-β-1,4-glucanase has been reported in GH10.

In this study, we report a GH10 endo-β-1,4-glucanase. *Arcticibacterium luteifluviistationis* SM1504^T is a bacterium isolated from Arctic seawater (17). A GH10 enzyme from the strain predicted by genomic annotation, which was named *A. luteifluviistationis* carboxymethyl cellulase (*Al*CMCase) in this study, was overexpressed in *Escherichia coli* and characterized. *Al*CMCase is a cold-adapted and salt-tolerant enzyme. Unlike other GH10 enzymes, *Al*CMCase displayed high endo-β-1,4-glucanase activity but negligible xylanase activity. Correspondingly, *Al*CMCase had remarkable binding capacities for cello-oligosaccharides rather than for xylo-oligosaccharides. These results indicate that *Al*CMCase is an endo-β-1,4-glucanase in GH10. Furthermore, *Al*CMCase and its homologs clustered as a group separate from the characterized GH10 xylanases in a phylogenetic tree, and two homologs of *Al*CMCase are also endo-β-1,4-glucanases. Therefore, we suggest that these enzymes represent a new subfamily of GH10 enzymes that have robust endo-β-1,4-glucanase activity.

RESULTS

***Al*CMCase is a member of GH10.** The gene encoding *Al*CMCase originated from the genome of strain SM1504^T, is 1,230 bp in length, and encodes a protein (*Al*CMCase) containing 409 amino acid residues. According to the predicted results from the NCBI Conserved Domain Database (CDD) and SignalP 4.1, *Al*CMCase contains a GH10 catalytic domain and a 19-residue signal peptide (Met1-Ala19). Based on amino acid sequence similarity, *Al*CMCase shows low identity to characterized xylanases, with the highest identity (35%; 88% coverage) to RsgI6-GH10 from *Clostridium thermocellum* by BLASTp against the UniProtKB database. RsgI6-GH10 is a modular protein that has low endo-β-1,4-xylanase activity and no cellulase activity (18). Compared to proteins with structural data in the Protein Data Bank (PDB) database, *Al*CMCase has the highest identity (26%; 72% coverage) to TmxB (PDB ID 1VBR) from *Thermotoga maritima*, which is a monospecific endo-β-1,4-xylanase containing only a GH10 catalytic domain (19). To further ascertain the relationship of *Al*CMCase to other GHs, we constructed a phylo-

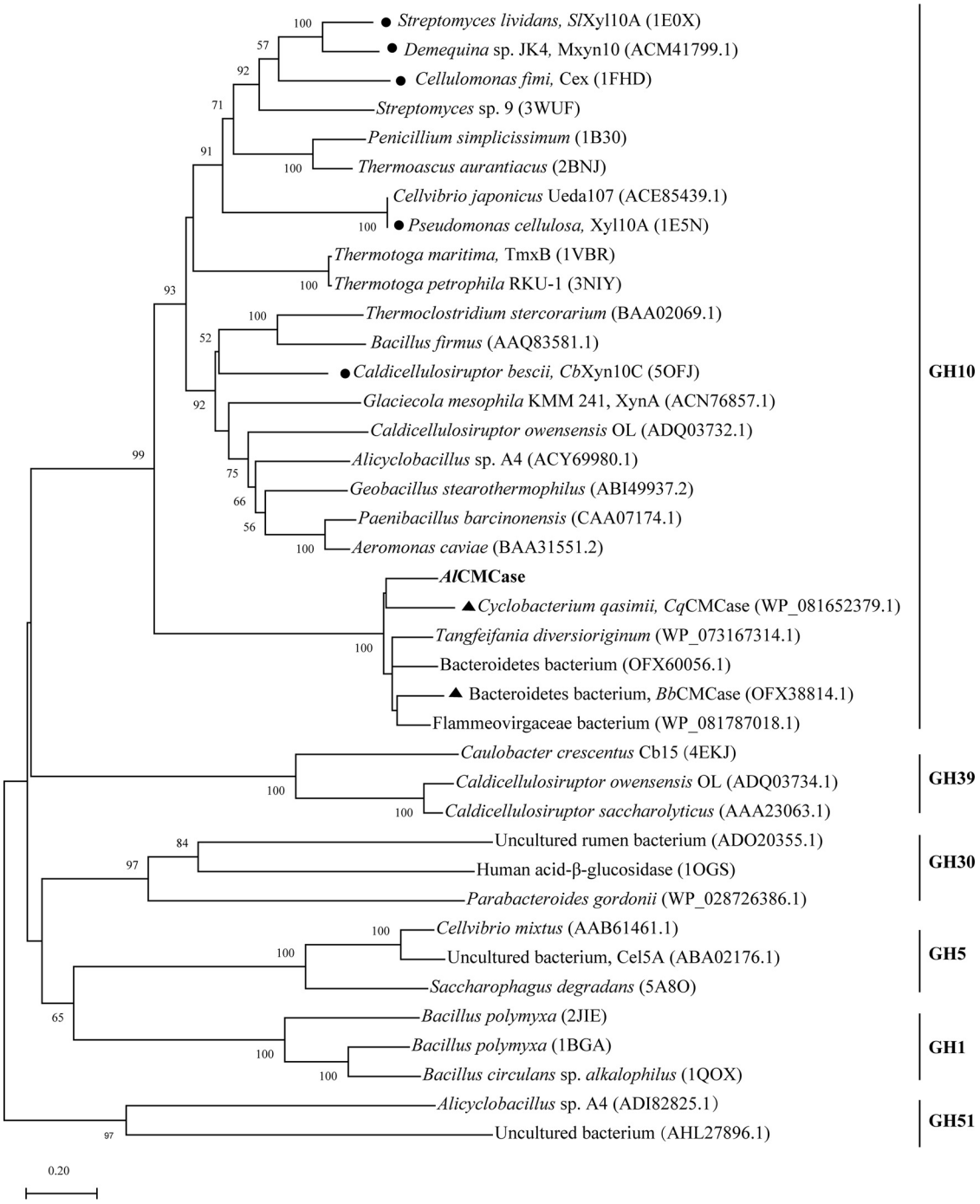

FIG 1 Phylogenetic analysis of *Al*CMCase and other enzymes from families GH1, -5, -10, -30, -39, and -51 in the GH-A clan. The tree was built by the neighbor-joining method with the Poisson model using 232 amino acid residues. A bootstrap test (500 replicates) was conducted, and values above 50% are shown. The circles indicate bifunctional xylanases/cellulases in GH10. The triangles indicate the homologs of *Al*CMCase characterized in this study.

genetic tree of *Al*CMCase and enzymes from GH1, -5, -10, -30, -39, and -51, because enzymes with xylanase or cellulase activity are reported only in these families in the GH-A clan. In the phylogenetic tree, *Al*CMCase and its homologs are clustered in a separate group and are more closely related to GH10 xylanases than to other GHs (Fig. 1), further suggesting that *Al*CMCase is a GH10 enzyme. To predict the catalytic residues of *Al*CMCase, multiple-sequence alignment was carried out with characterized mono-specific xylanases (TmxB, XynA [GenBank accession no. ACN76857.1] from *Glaciecola*

mesophila, and XynAS9 [PDB ID 3WUF] from *Streptomyces* sp.) and bifunctional xylanases/cellulases (*Cb*Xyn10C [PDB ID 5OFJ] from *Caldicellulosiruptor bescii*, Cex [PDB ID 1FHD] from *Cellulomonas fimi*, *Sl*Xyl10A [PDB ID 1E0X] from *Streptomyces lividans*, Xyl10A [PDB ID 1E5N] from *Pseudomonas cellulosa*, and Mxyn10 [GenBank accession no. ACM41799.1] from *Demequina* sp.) in GH10 and *Al*CMCase and its two homologs (*Bb*CMCase [GenBank accession no. MENL01000062.1] from *Bacteroidetes* bacterium GWB2_41_8 and *Cq*CMCase [GenBank accession no. ATNM01000137.1] from *Cyclobacterium qasimii* M12-11B). The result revealed that two conserved glutamate residues, Glu178 and Glu277 in *Al*CMCase, are likely to be the catalytic acid/base (Fig. 2). These two residues are also conserved in *Bb*CMCase and *Cq*CMCase. This result suggests that *Al*CMCase and its homologs probably adopt the same catalytic mechanism as other GH10 enzymes. Taken together, the data show that *Al*CMCase is a member of GH10 showing low identities to characterized xylanases and those with solved structures, which deserves to be studied in detail.

***Al*CMCase is a cold-adapted and salt-tolerant enzyme.** Recombinant *Al*CMCase was expressed in *E. coli* BL21(DE3) and purified. The SDS-PAGE analysis showed that *Al*CMCase had high purity and displayed an apparent molecular mass of approximately 45 kDa (Fig. 3A), consistent with its calculated molecular mass of 46.0 kDa. *Al*CMCase displayed extremely low xylanase activities on wheat arabinoxylan (WAX) (25.3 $\pm$ 0.6 U/μmol) and beechwood xylan (1.2 $\pm$ 0.1 U/μmol) but exhibited efficient hydrolysis on carboxymethyl cellulose (CMC) (615.6 $\pm$ 6.4 U/μmol) and hydroxyethyl cellulose (HEC) (386.0 $\pm$ 41.9 U/μmol) (Table 1). This result indicates that *Al*CMCase mainly possesses β-1,4-glucanase activity.

Using CMC as a substrate, we determined the biochemical characters of *Al*CMCase. *Al*CMCase displayed the highest activity at 40°C and pH 6.0 in phosphate-buffered saline (PBS) (Fig. 3B and C). While most of the tested metal ions and chemical reagents had no obvious effect on *Al*CMCase activity, 10 mM Fe^{2+} and Mn^{2+} increased its activity to 131.3% and 161.5%, respectively, and 10 mM sodium dodecyl sulfate (SDS) reduced its activity to 13.9% (Table 2). We also found that *Al*CMCase has properties of adaptation to Arctic seawater. *Al*CMCase retained 23.3% of its maximum activity at 0°C and 44.8% at 10°C (Fig. 3B), indicating that it is a cold-active enzyme. Furthermore, *Al*CMCase was quite thermally unstable. It lost almost all its activity after incubation at 35°C for 1 h or at 45°C for 3 min (Fig. 4A), and the thermal-unfolding temperature (T_m) of the enzyme was determined to be as low as 40.9°C (Fig. 4B). These results indicate that *Al*CMCase is a cold-adapted enzyme. In addition, NaCl can activate *Al*CMCase activity. *Al*CMCase showed the highest activity in 1.0 M NaCl (172.6% of the activity in 0 M NaCl) (Fig. 4C), and it still retained more than 80% of the enzyme activity in 5.0 M NaCl after incubation at 4°C for 24 h (Fig. 4D), indicating that it is a salt-active and salt-tolerant enzyme. Moreover, NaCl significantly improved the thermostability of *Al*CMCase. After incubation at 35°C for 30 min, *Al*CMCase retained only 26.1% activity in 0 M NaCl but more than 85% activity in 0.1 to 5.0 M NaCl (Fig. 4E), and its T_m increased from 40.9°C in 0 M NaCl to 47.4°C in 0.5 M NaCl (Fig. 4F). Altogether, *Al*CMCase is cold adapted and salt tolerant, well adapted to the cold and saline Arctic seawater where strain SM1504^T was isolated.

***Al*CMCase is an endo-β-1,4-glucanase with negligible xylanase activity.** To investigate the substrate specificity of *Al*CMCase, we measured its activity on a variety of cello- and xylo-configured substrates. The results showed that *Al*CMCase exhibited more than 15.3-fold higher activity on β-1,4-glucans than on β-1,4-xylans (Table 1). It showed no activity on Avicel (cellulose microcrystalline, from cotton linters), laminarin, lichenan, starch, p-nitrophenyl-β-D-glucopyranoside (pNPG), or p-nitrophenyl-β-D-xylopyranoside (pNPX), indicating that *Al*CMCase has no exo-β-1,4-glucanase, β-1,3-1,6-glucanase, β-1,3-1,4-glucanase, α-1,4-glucanase, β-1,4-glucosidase, or β-1,4-xylosidase activity (Table 1). Among CMC, HEC, and WAX, *Al*CMCase displayed the highest k_{cat} value and the lowest K_m value on CMC (Table 3; see Fig. S1 in the supplemental material), showing that *Al*CMCase had the highest catalytic efficiency on

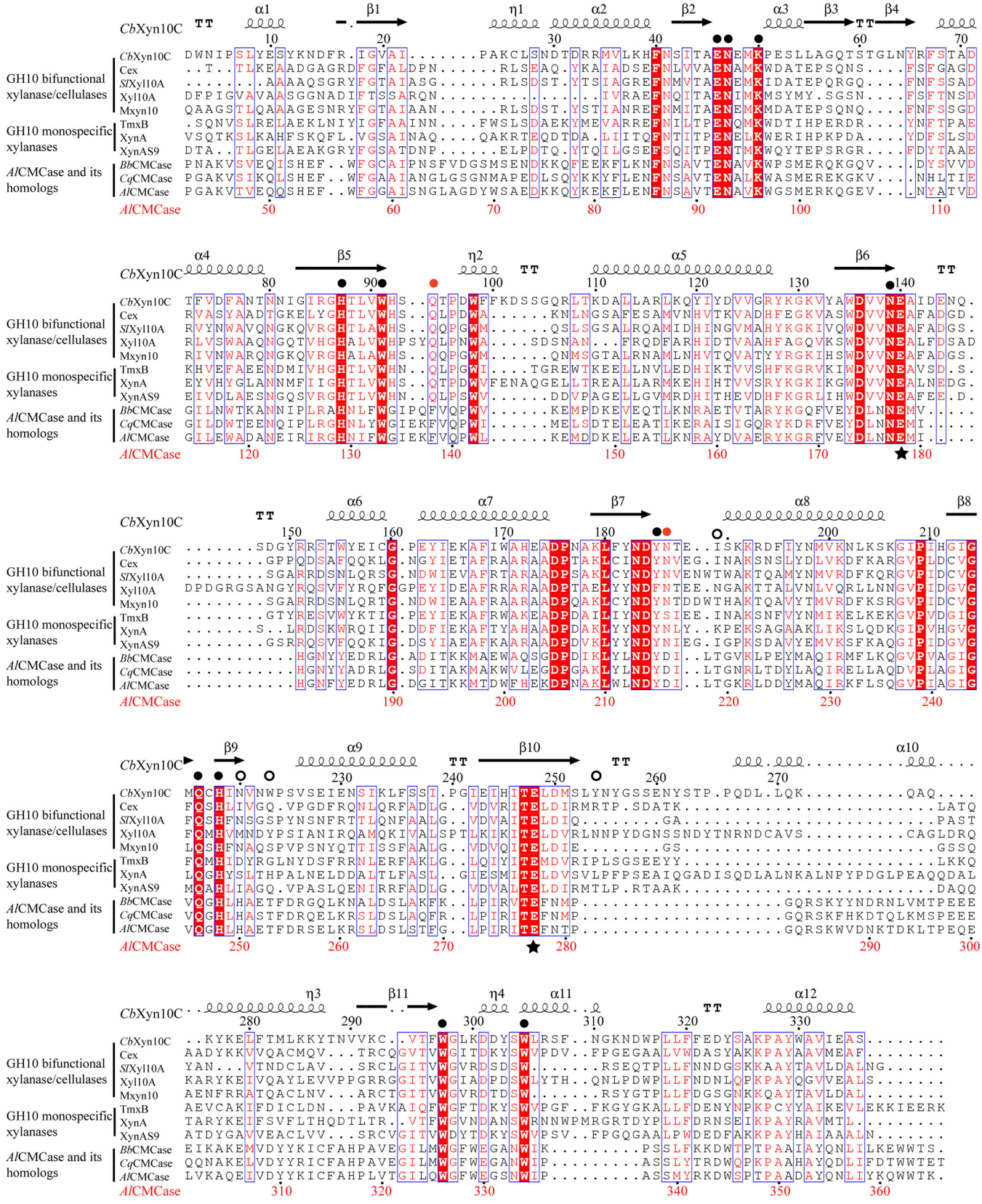

FIG 2 Amino acid sequence alignment of *Al*CMCase with other GH10 enzymes. The amino acid sequences were TmxB (PDB ID 1VBR) from *T. maritima*, XynA (GenBank accession no. ACN76857.1) from *G. mesophila*, XynAS9 (PDB ID 3WUF) from *Streptomyces* sp., Xyl10A (PDB ID 1E5N) from *P. cellulosa*, *Sl*Xyl10A (PDB ID 1E0X) from *S. lividans*, Cex (PDB ID 1FHD) from *C. fimi*, *Cb*Xyn10C (PDB ID 5OFJ) from *C. bescii*, Mxyn10 (GenBank accession no. ACM41799.1) from *Demequina* sp., *Al*CMCase in this study (GenBank accession no. WP_111373332.1) from *A. luteifluviistationis*, *Bb*CMCase (GenBank accession no. OFX60056.1) from

(Continued on next page)

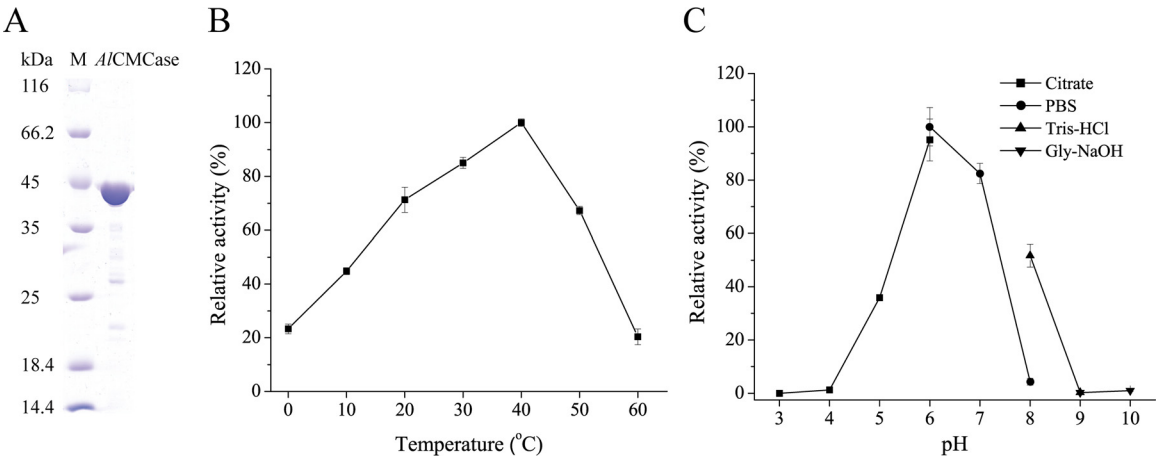

FIG 3 Biochemical characterization of *Al*CMCase. (A) SDS-PAGE analysis of purified *Al*CMCase. (B) Effect of temperature on *Al*CMCase activity. (C) Effect of pH on *Al*CMCase activity. The specific activity of *Al*CMCase determined at 40°C in PBS (378.5 ± 5.2 U/μmol [B] and 345.1 ± 25.6 U/μmol [C]) was taken as 100%. The data shown in the graphs are from triplicate experiments (means ± standard deviations [SD]).

CMC. The k_{cat}/K_m value of *Al*CMCase on CMC was 54.2-fold higher than that on WAX (Table 3; see Fig. S1). These results indicated that *Al*CMCase mainly acts on β-1,4-glycosidic linkages of cellulose with negligible xylanase activity.

We further analyzed the products released from cello-oligosaccharides (G_2 to G_6), CMC, xylo-oligosaccharides (X_2 to X_6), and WAX by the hydrolysis of *Al*CMCase with thin-layer chromatography (TLC). For cello-oligosaccharides, *Al*CMCase hydrolyzed cellotriose, cellotetraose, cellopentaose, and cellohexaose (G_3 to G_6), and the hydrolysis products were glucose and cellobiose. When it acted on CMC, in addition to glucose and cellobiose, oligosaccharides with higher degrees of polymerization (DP $>$ 2) were also observed (Fig. 5A), indicating that *Al*CMCase adopts an endoaction mode on cello-configured substrates. Similarly, the end products of xylo-oligosaccharides (X_3 to X_6) hydrolyzed by *Al*CMCase were xylose and xylobiose. Xylobiose and a few xylo-oligosaccharides (DP $>$ 2) were detected when WAX was hydrolyzed (Fig. 5B). These results indicated that *Al*CMCase hydrolyzes cellulose and xylan with the same mode, which adopts an endo-action pattern with a requirement for at least three glucose or xylose units for effective cleavage.

To analyze the binding capacity of *Al*CMCase for cello-oligosaccharides and xylo-oligosaccharides, we performed site-directed mutagenesis on the predicted catalytic residue Glu178 and obtained a mutant, E178Q, that showed no activity on CMC or WAX (Fig. 6). Then, the capacity of E178Q to bind cello-oligosaccharides (G_2 to G_5) and xylo-oligosaccharides (X_2 to X_5) was determined by isothermal titration calorimetry (ITC). The results showed that *Al*CMCase could bind cello-oligosaccharides (G_2 to G_5) but had no detectable capacity to bind to xylo-oligosaccharides (X_2 to X_5) (Fig. 7), which may explain why *Al*CMCase had negligible xylanase activity.

Therefore, by comparing the hydrolytic activities and binding capacities of *Al*CMCase for xylo- and cello-configured substrates, it can be concluded that *Al*CMCase is an endo-β-1,4-glucanase with negligible xylanase activity.

***Al*CMCase and its homologs form a new subfamily of endo-β-1,4-glucanases in GH10.** As shown in Fig. 1, *Al*CMCase and its homologs form a new branch in GH10. To

FIG 2 Legend (Continued)

Bacteroidetes bacterium GWB2_41_8, and *Cq*CMCase (GenBank accession no. EPR66937.1) from *C. qasimii* M12-11B. The catalytic domains of all the sequences were predicted with InterPro and used for alignment. Secondary structures and amino acid numbering for *Cb*Xyn10C (using ESPript) are shown above the alignment. Loops, arrows, TT, and η indicate helices, strands, turns, and 3_{10}-helices, respectively. Amino acid numbering for *Al*CMCase is shown below the alignment in red. The stars indicate conserved catalytic residues (Glu178 and Glu277 in *Al*CMCase) in GH10. In *Cb*Xyn10C, 17 residues interacting with xylo- or cello-oligosaccharides are marked with circles (solid for 13 conserved residues and open for 4 nonconserved residues). The red circles indicate 2 residues that are conserved in other GH10 enzymes but nonconserved in *Al*CMCase and its homologs.

TABLE 1 Substrate specificity of *Al*CMCase[a]

Substrate	Sp act (U/μmol)	Description
CMC	615.6 ± 6.4	Substrate for endo-β-1,4-glucanase
HEC	386.0 ± 41.9	Substrate for endo-β-1,4-glucanase
WAX	25.3 ± 0.6	Substrate for endo-β-1,4-xylanase
Beechwood xylan	1.2 ± 0.1	Substrate for endo-β-1,4-xylanase
Avicel	ND[b]	Substrate for exo-β-1,4-glucanase
Laminarin	ND	Substrate for β-1,3/1,6-glucanase
Lichenan	ND	Substrate for β-1,3-1,4-glucanase
Starch	ND	Substrate for α-1,4-glucanase
pNPG	ND	Substrate for β-1,4-glucosidase
pNPX	ND	Substrate for β-1,4-xylosidase

[a]The assays were carried out at 40°C in PBS containing 1.0 M NaCl. The substrates used were 12 mg/ml CMC, 24 mg/ml other polysaccharides, and 20 mM pNPG and pNPX. *Al*CMCase concentrations were 0.94 μmol for CMC and 4.70 μmol for other substrates. Reaction times were 10 min for CMC and HEC, 1 h for WAX, and 12 h for other substrates.
[b]ND, enzyme activity was not detectable.

analyze whether other enzymes in this branch are also endo-β-1,4-glucanases, two homologs of *Al*CMCase, *Bb*CMCase and *Cq*CMCase, were characterized. With CMC as a substrate, *Bb*CMCase showed the highest activity at 40°C in citrate buffer (pH 6.0) containing 0.1 M NaCl (see Fig. S2A in the supplemental material), and *Cq*CMCase showed the highest activity at 40°C in citrate buffer (pH 6.0) containing 1.0 M NaCl (see Fig. S2B). At their respective optimum temperatures, pHs, and NaCl concentrations, the activities of *Bb*CMCase and *Cq*CMCase on CMC and WAX were determined. Similar to *Al*CMCase, both *Bb*CMCase and *Cq*CMCase showed high activity on CMC and extremely low activity on WAX (Table 4). The ratios of k_{cat}/K_m (CMC) to k_{cat}/K_m (WAX) for *Bb*CMCase and *Cq*CMCase were 47.4 and 33.3, respectively, which were similar to that for *Al*CMCase (54.2) (Table 4; see Fig. S3 in the supplemental material). Therefore, *Al*CMCase and its two homologs have the same substrate specificity, and all predominantly function as endo-β-1,4-glucanases. Based on these results, we suggest that *Al*CMCase and its homologs form a new subfamily of GH10 enzymes that have robust endo-β-1,4-glucanase activity.

DISCUSSION

The well-studied GH10 bifunctional xylanases/cellulases include Xyl10A (13), *Sl*Xyl10A (14), Cex (15), and *Cb*Xyn10C (16). To compare the catalytic efficiencies of

TABLE 2 Effects of metal ions and chemical reagents on *Al*CMCase activity[a]

Metal ion or chemical reagent[b]	Relative activity (%) at:	
	1 mM	10 mM
Mg^{2+}	103.9 ± 8.7	113.8 ± 0.4
Li^{2+}	104.7 ± 8.4	100.8 ± 0.44
Ca^{2+}	107.1 ± 3.9	100.8 ± 0.44
Zn^{2+}	105.9 ± 5.2	112.9 ± 10.2
K^{+}	119.2 ± 5.2	112.7 ± 1.0
Ni^{2+}	105.9 ± 2.9	102.4 ± 6.4
Ba^{2+}	118.4 ± 5.4	114.0 ± 1.8
Co^{2+}	116.8 ± 3.2	109.9 ± 3.9
Cu^{2+}	106.4 ± 8.6	88.3 ± 2.1
Fe^{2+}	109.7 ± 2.2	131.3 ± 2.6
Mn^{2+}	102.2 ± 2.1	161.5 ± 4.1
DTT	112.6 ± 3.2	113.8 ± 8.2
Urea	114.5 ± 4.8	104.5 ± 7.1
2-Mercaptoethanol	97.8 ± 4.35	92.1 ± 3.1
Thiourea	111.6 ± 6.4	100.8 ± 5.2
EDTA	106.3 ± 2.6	79.2 ± 0.34
SDS	78.6 ± 4.5	13.9 ± 1.0

[a]*Al*CMCase activity was determined at 40°C in PBS containing the metal ion or chemical regent at a final concentration of 1 mM or 10 mM. The specific activity of *Al*CMCase under the same conditions without the addition of the metal ion or chemical regent (388.1 ± 12.9 U/μmol) was taken as 100%.
[b]DTT, dithiothreitol.

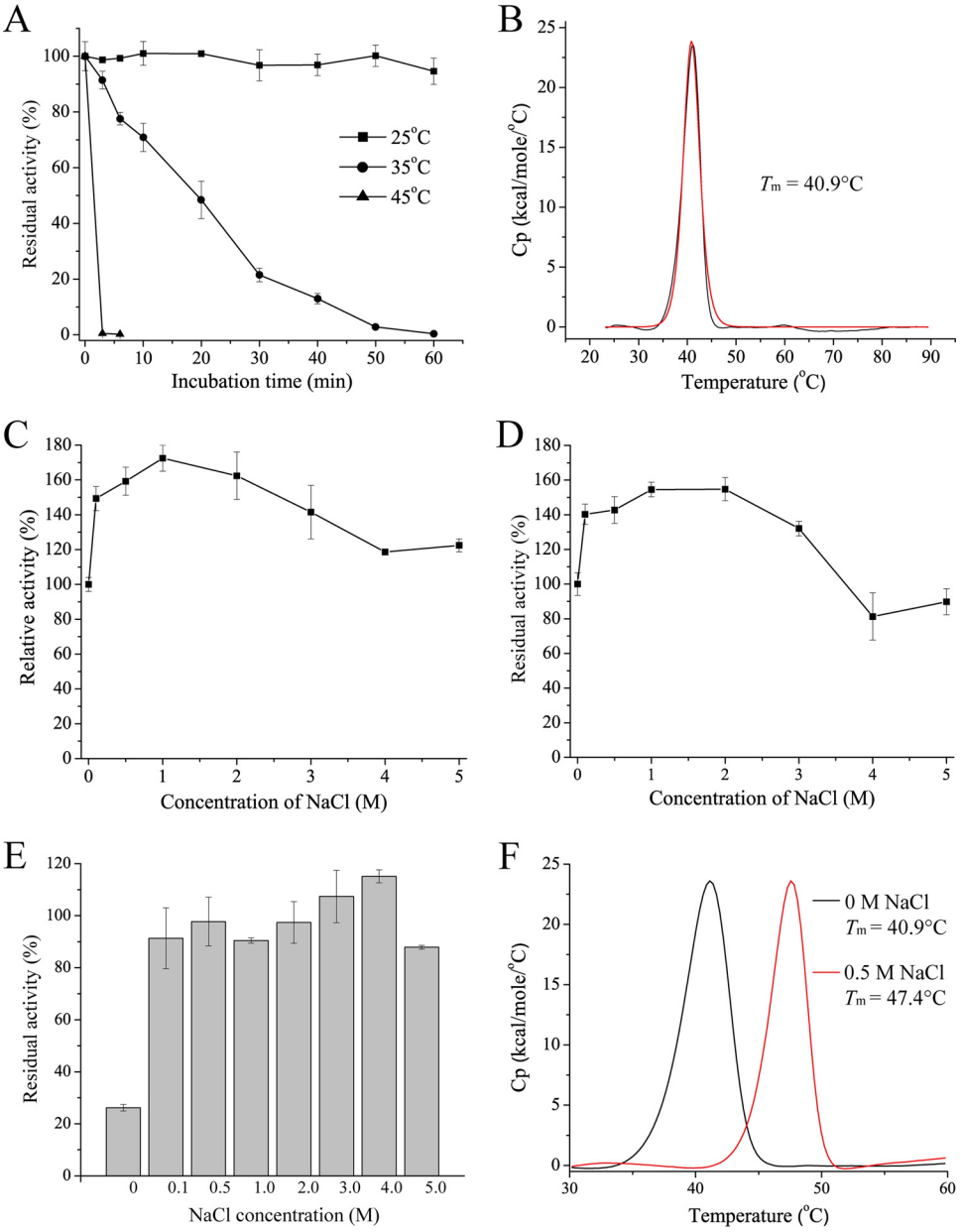

FIG 4 Properties of *Al*CMCase adaptation to Arctic seawater. (A) Effect of temperature on *Al*CMCase stability. *Al*CMCase was incubated at 25°C, 35°C, and 45°C for different periods. The residual activity was determined at 40°C and pH 6.0. The specific activity of *Al*CMCase incubated at 4°C (415.9 ± 21.6 U/μmol) was taken as 100%. (B) Determination of the T_m of *Al*CMCase. The T_m was determined by DSC as the temperature increased from 20°C to 90°C at a heating rate of 1°C/min. The red line represents the fitting curve of the initial data. (C) Effect of NaCl on *Al*CMCase activity. The specific activity of *Al*CMCase in 0 M NaCl (453.7 ± 18.1 U/μmol) was taken as 100%. (D) Effect of NaCl on *Al*CMCase stability. The residual activity was determined after incubating *Al*CMCase in 0 to 5.0 M NaCl at 4°C for 24 h. The specific activity of *Al*CMCase in 0 M NaCl (438.6 ± 29.9 U/μmol) was taken as 100%. (E) Effect of NaCl on *Al*CMCase thermostability. *Al*CMCase in PBS containing 0 to 5.0 M NaCl was incubated at 35°C for 30 min. The residual activity was determined at 40°C and pH 6.0. The specific activities of *Al*CMCase in the corresponding concentrations of NaCl incubated at 4°C were taken as 100%. (F) Comparison of the T_m values of *Al*CMCase incubated with and without 0.5 M NaCl. The data shown in the graph are from triplicate experiments (means ± SD).

these enzymes on xylan and cellulose, we calculated the ratios of k_{cat}/K_m (xylan) to k_{cat}/K_m (cellulose) based on the kinetic parameters reported in the literature. With aryl glycosides as substrates, the ratios of k_{cat}/K_m (p-nitrophenyl-β-D-xylobiose [pNPX2]) to k_{cat}/K_m (p-nitrophenyl-β-D-cellobiose [pNPG2]) for Xyl10A, *Sl*Xyl10A, and Cex were 2,915, 714, and 83, respectively (Table 5) (13–15). This indicates that these bifunctional

TABLE 3 Kinetic parameters of *Al*CMCase on CMC, HEC, and WAX[a]

Substrate	V_{max} (μmol/min/μmol of enzyme)	k_{cat} (s^{-1})	K_m (mg/ml)	k_{cat}/K_m (s^{-1} mg/ml^{-1})
CMC	830.0 ± 38.8	13.8 ± 0.65	5.3 ± 0.5	2.60
HEC	482.6 ± 25.3	8.0 ± 0.4	11.5 ± 1.0	0.70
WAX	39.5 ± 1.8	0.66 ± 0.03	14.6 ± 1.1	0.048

[a]Kinetic parameters were calculated by nonlinear regression fitted directly to the Michaelis-Menten equation using Origin8 software. The initial rates were determined with 0 to 24 mg/ml CMC, 0 to 42 mg/ml HEC, and 0 to 32 mg/ml WAX. The nonlinear fit curves for the hydrolysis of CMC, HEC, and WAX by *Al*CMCase are shown in Fig. S1.

xylanases/cellulases hydrolyze xylan more efficiently than they hydrolyze cellulose. With polysaccharides as substrates, the differences are even more significant. The catalytic efficiency of Cex on soluble oat spelt xylan (OSX) is more than 10,000-fold higher than that on CMC (13), similar to the difference observed for *Cb*Xyn10C on WAX and CMC (Table 5) (16). Thus, these bifunctional GH10 xylanases/cellulases have robust xylanase activity. Up to now, no endo-β-1,4-glucanase has been reported in GH10. In this study, we found that *A. luteifluviistationis Al*CMCase, which is a GH10 enzyme based on sequence alignment, functions as an endo-β-1,4-glucanase that can efficiently hydrolyze β-1,4-linked CMC, HEC, and cello-oligosaccharides (DP > 2). However, *Al*CMCase has extremely low xylanase activity. Compared to *Cb*Xyn10C (39,000 U/μmol), *Al*CMCase showed 32,500-fold lower activity (1.2 U/μmol) on beechwood xylan and 2,015-fold lower activity (51,000 U/μmol for *Cb*Xyn10C versus 25.3 U/μmol for *Al*CMCase) and 49-fold higher K_m (0.3 mg/ml for *Cb*Xyn10C versus 14.6 mg/ml for *Al*CMCase)

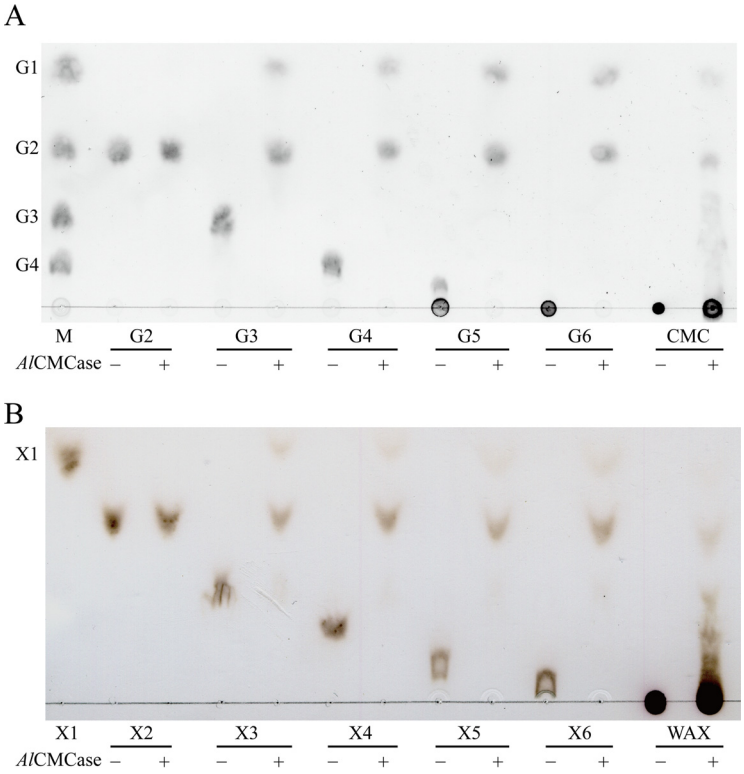

FIG 5 TLC analysis of the products released from cello- and xylo-configured substrates by the hydrolysis of *Al*CMCase. (A) Products from cello-oligosaccharides and CMC. (B) Products from xylo-oligosaccharides and WAX. Each cello-configured substrate was incubated with *Al*CMCase at 25°C for 12 h, and each xylo-configured substrate was incubated with *Al*CMCase at 25°C for 36 h. The products were analyzed by TLC. Lanes: M, a mixture of authentic cello-oligosaccharides; G_1, glucose; G_2, cellobiose; G_3, cellotriose; G_4, cellotetraose; G_5, cellopentaose; G_6, cellohexaose; X_1, xylose; X_2, xylobiose; X_3, xylotriose; X_4, xylotetraose; X_5, xylopentaose; X_6, xylohexaose. The data are representative of the results of triplicate experiments.

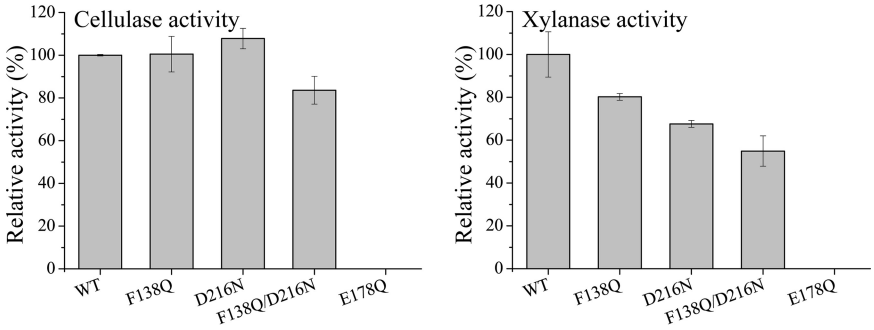

FIG 6 Activities of *Al*CMCase mutants on CMC and WAX. The reaction mixture for cellulase activity contained 0.94 μM enzyme and 12 mg/ml CMC, and that for xylanase activity contained 4.70 μM enzyme and 24 mg/ml WAX in PBS containing 1.0 M NaCl. The specific activity of wild-type (WT) *Al*CMCase (600.6 $\pm$ 12.8 U/μmol on CMC or 23.7 $\pm$ 0.1 U/μmol on WAX) was taken as 100%. The error bars indicate SD.

on WAX (Tables 1 and 3) (16). In contrast, with CMC as the substrate, the specific activity of *Al*CMCase was in the range of 345.1 to 615.6 U/μmol, which is comparable to those of the GH5 cellulases metagenome-derived Cel5A (2,863 U/μmol), CelE1 (600 U/μmol), and *Volvariella volvacea* EG1 (1,470 U/μmol) (Table 5) (20–22) and much higher than those of Cex (3.1 U/μmol) (15) and *Cb*Xyn10C (39 U/μmol) (16). These data indicate that *Al*CMCase is a GH10 cellulase rather than a xylanase.

It has been reported that *Cb*Xyn10C has effective binding capacity for xylo-oligosaccharides (X_2 to X_6) (23), similar to two GH10 monospecific xylanases, XT6 and IXT6, from *Geobacillus stearothermophilus* T-6 (24), and the binding capacity of *Cb*Xyn10C for xylo-oligosaccharides was much stronger than that for cello-oligosaccharides (G_5 to G_6) (23). This is consistent with *Cb*Xyn10C being a robust xylanase. In contrast to these xylanases, *Al*CMCase shows remarkable binding capacity for cello-oligosaccharides (G_2 to G_5) and no detectable binding capacity for xylo-oligosaccharides (X_2 to X_5) (Fig. 7), implying that the substrate binding pocket of *Al*CMCase is more suitable for cellulose substrate. Structural analysis showed that Gln94 and Trp305 in *Cb*Xyn10C form a steric hindrance for cellulose substrate due to the additional hydroxymethyl of glucose at C-6 (16, 23), just as in the cases of Xyl10A, *Sl*Xyl10A, and Cex (13–15). This hindrance results in the poor binding of these enzymes to cellulose, leading to their negligible cellulase activity (13–15, 23). In *Cb*Xyn10C, 17 residues have been shown to interact with xylo- or cello-oligosaccharides via hydrogen bonding or hydrophobic stacking (23). Among these residues, 13 residues are conserved or relatively conserved in GH10 enzymes and 4 residues are not conserved (Fig. 2). The conserved residues play important roles in the hydrolysis of xylan or cellulose (23). Sequence alignment showed that the conserved Gln94 (in *Cb*Xyn10C) has a counterpart in phenylalanine (Phe138 in *Al*CMCase) and Asn186 (in *Cb*Xyn10C) has a counterpart in aspartic acid (Asp216 in *Al*CMCase) in *Al*CMCae and its homologs (Fig. 2). However, when site-directed mutagenesis was performed on Phe138 and Asp216 in *Al*CMCase, no increased xylanase activity was detected in the F138Q, D216N, or F138Q/D216N mutant (Fig. 6). Thus, there should be other structural elements in *Al*CMCase related to the poor binding capacity for xylo-oligosaccharides, which needs further study based on structural analysis in the future.

We found that two homologs of *Al*CMCase have the same substrate specificity as *Al*CMCase, both mainly having β-1,4-glucanase activity. Because *Al*CMCase and its homologs are grouped into an independent branch in the phylogenetic tree of GH10 enzymes (Fig. 1), we suggest that these enzymes form a new subfamily of GH10 enzymes that have robust endo-β-1,4-glucanase activity.

It has been reported that certain metal ions can increase the activity of some glycoside hydrolases. For example, the activity of the xylanase XynB from *Xanthomonas axonopodis* pv. *citri* was activated by Ca^{2+} and Mg^{2+} (25), the activity of the xylosidase

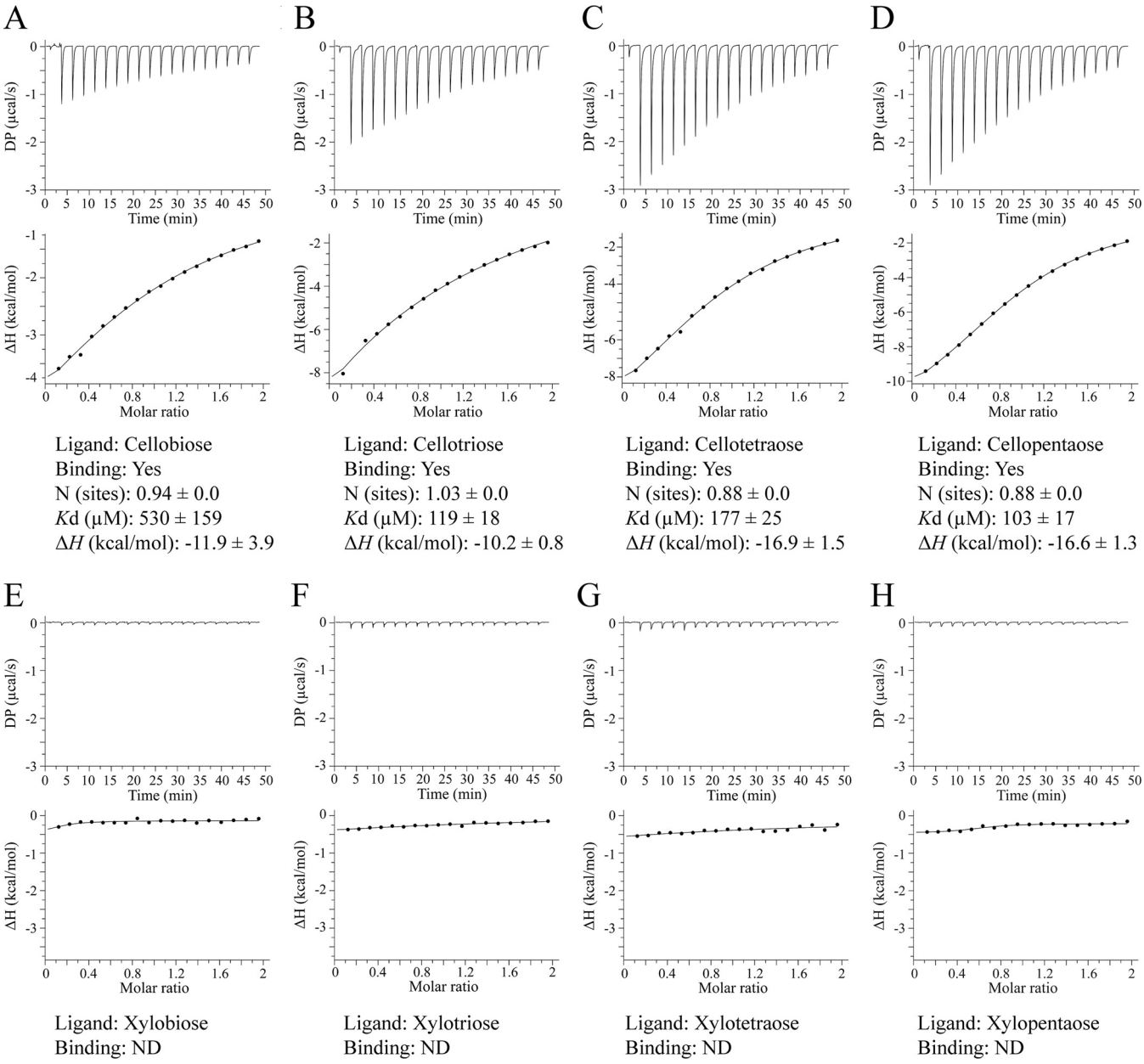

FIG 7 ITC analysis of the capacity of the inactive E178Q mutant to bind to cello-oligosaccharides (G_2 to G_5) and xylo-oligosaccharides (X_2 to X_5). The experiment was carried out at 25°C in 50 mM Tris-HCl (pH 7.0) containing 1.0 M NaCl. The concentrations of E178Q and oligosaccharides were 0.25 mM and 2.5 mM, respectively. ND indicates no detectable binding capacity. Data representative of the results of triplicate experiments are shown.

rSWU43A from *Streptomyces* sp. strain SWU10 was activated by Fe^{2+} and Mn^{2+} (26), and the activity of the metagenome-derived cellulase CellMM5.1 was activated by Mn^{2+} and Co^{2+} (27). In this study, we found that Fe^{2+} and Mn^{2+} increased *Al*CMCase activity (Table 2). In addition, as an Arctic marine-derived enzyme, *Al*CMCase possesses potential attractiveness for industrial applications. It has cold-adapted and salt-tolerant properties, suggesting that it may be a candidate biocatalyst for industrial processes under low temperature or high salinity, such as seafood and saline-food processing.

MATERIALS AND METHODS

Materials and strains. CMC, hydroxyethyl cellulose, beechwood xylan, Avicel, laminarin, starch, pNPG, pNPX, glucose, cellobiose, and xylose were purchased from Sigma (St. Louis, MO). WAX, lichenan, cello-oligosaccharides (G_3 to G_6), and xylo-oligosaccharides (X_2 to X_6) were purchased from Megazyme (Ireland). *A. luteifluviistationis* SM1504^T (GenBank accession no. CP029480.1) was previously isolated from

TABLE 4 Comparison of the substrate specificities and kinetic parameters of *Al*CMCase and its homologs[a]

Protein	CMC				WAX			
	Sp act (U/μmol)	K_m (mg/ml)	k_{cat} (s^{-1})	k_{cat}/K_m (s^{-1} mg/ml^{-1})	Sp act (U/μmol)	K_m (mg/ml)	k_{cat} (s^{-1})	k_{cat}/K_m (s^{-1} mg/ml^{-1})
*Al*CMCase	615.6 ± 6.4	5.3 ± 0.5	13.8 ± 0.6	2.60	25.3 ± 0.6	14.6 ± 1.2	0.66 ± 0.03	0.048
*Bb*CMCase	809.8 ± 17.9	4.5 ± 0.2	14.7 ± 0.4	3.27	42.9 ± 1.2	12.7 ± 3.4	0.88 ± 0.15	0.069
*Cq*CMCase	359.8 ± 27.2	4.0 ± 0.3	6.5 ± 0.3	1.63	30.7 ± 1.4	12.4 ± 1.9	0.61 ± 0.07	0.049

[a]Two homologs of *Al*CMCase are *Bb*CMCase (GenBank accession no. OFX60056.1) from *Bacteroidetes* bacterium GWB2_41_8 and *Cq*CMCase (GenBank accession no. EPR66937.1) from *C. qasimii* M12-11B. Nonlinear fit curves for the hydrolysis of CMC and WAX by *Cq*CMCase and *Bb*CMCase are shown in Fig. S3.

Arctic seawater (17). The strain was grown in Difco marine broth 2216 (Becton, Dickinson) at 20°C. *E. coli* DH5α and *E. coli* BL21(DE3) (TransGen Biotech, China) were used for plasmid construction and gene expression, respectively. They were grown in Luria-Bertani (LB) medium at 37°C.

Gene cloning, mutation, and enzyme expression and purification. The gene that encodes *Al*CMCase (GenBank accession no. WP_111373332.1) was cloned from the genomic DNA of SM1504^T by PCR amplification and inserted into the pET22b vector (Novagen, USA). Using pET22b-*alCMCase* as the template, site-directed mutation was introduced with the QuikChange mutagenesis kit II (Agilent Technologies, USA) to construct E178Q, F138Q, D216N, and F138Q/D216N mutants. The primers used are shown in Table 6. The genes encoding *Bb*CMCase from *Bacteroidetes* bacterium GWB2_41_8 (GenBank accession no. MENL01000062.1), and *Cq*CMCase from *C. qasimii* M12-11B (GenBank accession no. ATNM01000137.1) without the predicted signal peptide were synthesized in the Beijing Genomics Institute (BGI) (Beijing, China) and inserted into pET22b. The constructed plasmids were transferred into *E. coli* BL21(DE3). The cells were cultured in LB medium containing 100 μg/ml ampicillin to an optical density at 600 nm (OD_{600}) of 0.8 to 1.0 and then induced by 0.5 mM isopropyl-β-D-thiogalactopyranoside (IPTG) at 20°C for 16 h. The cells were harvested and disrupted with high pressure. Then, recombinant proteins were purified by nickel chromatography on an Ni^{2+}-nitrilotriacetic acid (NTA) column (GE Healthcare, USA) and gel filtration on a Superdex G200 column (GE Healthcare, USA). The purities of enzymes were determined by SDS-PAGE.

Enzyme assay. *Al*CMCase activities on xylo- and cello-configured polysaccharides were determined by the dinitrosalicylic acid (DNS) method (28). For cello-configured polysaccharides, the 125-μl reaction mixture contained 0.94 μM *Al*CMCase and 12 mg/ml polysaccharide in PBS (pH 6.0, containing 6.15 mM NaH_2PO_4 and 43.85 mM Na_2HPO_4). After incubation at 40°C for 10 min, the reaction was terminated by the addition of 100 μl DNS, and the reaction mixture was boiled for coloring. Then, the absorbance at 550 nm was measured. When p-nitrophenyl (pNP) derivatives, pNPG and pNPX, were used as substrates, the 100-μl reaction mixture contained 4.70 μM *Al*CMCase and 20 mM pNPG or pNPG in PBS. After incubation at 40°C for 10 min, 600 μl Na_2CO_3 was added, and the absorbance at 405 nm was measured. For xylo-configured polysaccharides, the reaction system contained an additional 1.0 M NaCl, and the *Al*CMCase concentration and the reaction time were increased to detect the extremely low activity of *Al*CMCase on these substrates. The activities of *Bb*CMCase and *Cq*CMCase on CMC and WAX were also determined by the DNS method in citrate buffer (pH 6.0, containing 9.50 mM citric acid and 40.50 mM sodium citrate) at 40°C and their respective optimum NaCl concentrations. One unit of enzyme activity is defined as the amount of enzyme required to release 1 μmol glucose, xylose, or p-nitrophenol per min. The protein concentration was determined by the bicinchoninic acid (BCA) method using a BCA protein assay kit (Thermo, USA) with bovine serum albumin (BSA) as the standard.

Biochemical characterization. The substrate specificity of *Al*CMCase was determined with the following polysaccharides: CMC, hydroxyethyl cellulose, WAX, beechwood xylan, Avicel, laminarin, lichenan, and starch, as well as pNPG and pNPX, at 40°C in PBS containing 1.0 M NaCl. The optimum temperature for *Al*CMCase activity was determined to range from 0°C to 60°C at intervals of 10°C. The

TABLE 5 Comparison of the substrate specificities of *Al*CMCase, GH10 monospecific xylanases, GH10 bifunctional xylanase/cellulases, and GH5 cellulases

GH family	Enzyme activity	Enzyme	Description[a]	Reference
GH10	Monospecific xylanase	XynA	3,300 U/μmol on beechwood xylan	33
		TmxB	1.84×10^5 U/μmol on OSX	34
	Bifunctional xylanase/cellulase	Xyl10A	$(k_{cat}/K_m$ [pNPX2])/$(k_{cat}/K_m$ [pNPG2]) = 2,915	13
		*Sl*Xyl10A	$(k_{cat}/K_m$ [pNPX2])/$(k_{cat}/K_m$ [pNPG2]) = 714	14
		Cex	$(k_{cat}/K_m$ [pNPX2])/$(k_{cat}/K_m$ [pNPG2]) = 83	15
			$(k_{cat}/K_m$ [OSX])/$(k_{cat}/K_m$ [CMC]) > 10,000	13
		*Cb*Xyn10C	$(k_{cat}/K_m$ [WAX])/$(k_{cat}/K_m$ [CMC]) = 8,800	16
	Bifunctional cellulase/xylanase	*Al*CMCase	$(k_{cat}/K_m$ [WAX])/$(k_{cat}/K_m$ [CMC]) = 0.018	
			345.1 to 615.6 U/μmol on CMC	
GH5	Cellulase	Cel5A	2,863 U/μmol on CMC	20
		CelE1	600 U/μmol on CMC	21
		EG1	1,470 U/μmol on CMC	22

[a]One unit of enzyme activity is the amount of enzyme that liberates 1 μmol of reducing group (xylose, glucose, or p-nitrophenol) per min.

TABLE 6 Primers used in this study

Gene product	Primer	Sequence (5′ to 3′)[a]
*Al*CMCase	*Al*CMCase-F	AAGAAGGAGATATACATATGCAATACGAAGGCATTGAAAA
	*Al*CMCase-R	TGGTGGTGGTGGTGCTCGAGGAACTCAACTTCTACCCTAC
E178Q	E178Q-F	GTCTTCATAAAAATTGCCATGAATCATCTGGTTGTTTAGATCATATTCTACAAAACG
	E178Q-R	CGTTTTGTAGAATATGATCTAAACAACCAGATGATTCATGGCAATTTTTATGAAGAC
F138Q	F138Q-F	TTCTTTGAGCCAAGGCTGCACCTGCTTCTCAATGCCCCAAAAGAT
	F138Q-R	ATCTTTTGGGGCATTGAGAAGCAGGTGCAGCCTTGGCTCAAAGAA
D216N	D216N-F	CGTTTTCCTGTCAGAATATTATAATCGTTTAACCATAACTTGGCATTTGG
	D216N-R	CCAAATGCCAAGTTATGGTTAAACGATTATAATATTCTGACAGGAAAACG

[a]Sequences identical to that of vector pET22b are underlined.

optimum pH for *Al*CMCase activity was determined to be from pH 3.0 to pH 11.0. The buffers used were 50 mM citrate buffer at pH 3.0 to 6.0, 50 mM PBS at pH 6.0 to 8.0, 50 mM Tris-HCl at pH 8.0 to 9.0, and 50 mM glycine-NaOH at pH 9.0 to 10.0. To analyze the effects of metal ions and chemicals on *Al*CMCase activity, each ion or chemical reagent was added to the reaction mixture at final concentrations of 1 mM and 10 mM. Then, the *Al*CMCase activity was determined at 40°C and pH 6.0. For the thermal-stability assay, residual activity was determined at 40°C and pH 6.0 after incubation of *Al*CMCase at 25°C, 35°C, or 45°C for different periods. The effect of NaCl on *Al*CMCase activity was determined in 0 to 5.0 M NaCl. For the halotolerance assay, *Al*CMCase was incubated in 0 to 5.0 M NaCl at 4°C for 24 h before the residual activity was determined at 40°C and pH 6.0. The thermal-unfolding (T_m) value of 1.0 mg/ml *Al*CMCase was determined as the temperature increased from 20°C to 90°C at a heating rate of 1°C/min by differential scanning calorimetry (DSC) on a MicroCal VP-Capillary DSC (Malvern, United Kingdom). Kinetic parameters were determined by nonlinear curve fitting based on the Michaelis-Menten equation using Origin8 software. The initial reaction rates were assayed with 0 to 24 mg/ml CMC or 0 to 32 mg/ml WAX at 40°C in PBS containing 1.0 M NaCl. The optimum temperatures, pHs, and NaCl concentrations and the kinetic parameters of *Bb*CMCase and *Cq*CMCase were determined by the same methods as for *Al*CMCase. Each experiment was performed in triplicate independently.

Thin-layer chromatography. Cello-oligosaccharides (G_2 to G_6; 0.4 mg/ml each) and CMC (0.4 mg/ml) were incubated with 8.7 μM *Al*CMCase in PBS at 25°C for 12 h. The products were then concentrated and analyzed by TLC. Xylo-oligosaccharides (X_2 to X_6; 2.5 mg/ml each) and WAX (10 mg/ml) were incubated with 108.9 μM *Al*CMCase in PBS containing 1.0 M NaCl at 25°C for 36 h. Before TLC analysis, the enzyme was removed from the reaction mixture by ultrafiltration. The solvent system in TLC analysis was 1-butanol–acetic acid–pure water (13:12:2 [vol/vol/vol]). Oligosaccharides were visualized by heating silica gel plates (Sigma, USA) at 100°C for 10 min after spraying with sulfuric acid-ethanol (1:10 [vol/vol]).

Isothermal titration calorimetry. ITC measurements were performed using MicroCal PEAQ-ITC (Malvern, United Kingdom) at 25°C. The concentrations of E178Q and oligosaccharides were 0.25 mM and 2.5 mM, respectively, in 50 mM Tris-HCl (pH 7.0) containing 1.0 M NaCl. Each oligosaccharide was injected into the protein cell 19 times with a stirring speed of 800 rpm (23, 24). The data were analyzed with Microcal PEAQ-ITC analysis software.

Bioinformatics. The signal peptide of *Al*CMCase was predicted by the SignalP 4.1 server (29), and domain analysis was performed in the NCBI Conserved Domain Database (30) and InterPro (http://www.ebi.ac.uk/interpro/). The molecular masses of proteins were calculated by ExPASy (https://www.expasy.org/). Multiple-amino-acid sequence alignment was carried out with CLC Sequence Viewer 6 and ESPript 3.0 (31). The phylogenetic tree was built with MEGA7 (32).

SUPPLEMENTAL MATERIAL

Supplemental material for this article may be found at https://doi.org/10.1128/AEM.01029-19.

SUPPLEMENTAL FILE 1, PDF file, 0.4 MB.

ACKNOWLEDGMENTS

The work was supported by the National Key R&D Program of China (grants 2018YFC1406700, 2018YFC1406704, and 2018YFC1406706), the National Science Foundation of China (grants 31670063, 31670038, 41676180, 91751101, U1706207, 31800107, and 91851205), the AoShan Talents Cultivation Program supported by the Qingdao National Laboratory for Marine Science and Technology (2017ASTCP-OS14 and QNLM2016ORP0310), the Taishan Scholars Program of Shandong Province (2009TS079), and the Young Scholars Program of Shandong University (2017WLJH57).

We declare that we have no conflicts of interest with the contents of this article.

F.Z., X.-L.C., and P.-Y.L. designed and directed the research. F.Z., H.-Y.C., and L.-S.Z. performed the experiments. X.-L.C. and F.Z. wrote the manuscript. Y.Z., P.W., C.-Y.L., and Y.-Z.Z. helped to analyze data and revise the manuscript.

REFERENCES

1. Usov AI, Zelinsky ND. 2013. Chemical structures of algal polysaccharides, p 23–86. *In* Dominguez H (ed), Functional ingredients from algae for foods and nutraceuticals. Elsevier, Cambridge, UK.
2. Sharma A, Tewari R, Rana SS, Soni R, Soni SK. 2016. Cellulases: classification, methods of determination and industrial applications. Appl Biochem Biotechnol 179:1346–1380. https://doi.org/10.1007/s12010-016-2070-3.
3. Nguyen STC, Freund HL, Kasanjian J, Berlemont R. 2018. Function, distribution, and annotation of characterized cellulases, xylanases, and chitinases from CAZy. Appl Microbiol Biotechnol 102:1629–1637. https://doi.org/10.1007/s00253-018-8778-y.
4. Collins T, Gerday C, Feller G. 2005. Xylanases, xylanase families and extremophilic xylanases. FEMS Microbiol Rev 29:3–23. https://doi.org/10.1016/j.femsre.2004.06.005.
5. Suenaga H. 2015. Targeted metagenomics unveils the molecular basis for adaptive evolution of enzymes to their environment. Front Microbiol 6:1018. https://doi.org/10.3389/fmicb.2015.01018.
6. De Santi C, Altermark B, de Pascale D, Willassen NP. 2016. Bioprospecting around Arctic islands: marine bacteria as rich source of biocatalysts. J Basic Microbiol 56:238–253. https://doi.org/10.1002/jobm.201500505.
7. Li PY, Yao QQ, Wang P, Zhang Y, Li Y, Zhang YQ, Hao J, Zhou BC, Chen XL, Shi M. 2017. A novel subfamily esterase with a homoserine transacetylase-like fold but no transferase activity. Appl Environ Microbiol 83:e00131-17. https://doi.org/10.1128/AEM.00131-17.
8. Lombard V, Golaconda Ramulu H, Drula E, Coutinho PM, Henrissat B. 2014. The Carbohydrate-Active Enzymes database (CAZy) in 2013. Nucleic Acids Res 42:D490–D495. https://doi.org/10.1093/nar/gkt1178.
9. Pollet A, Delcour JA, Courtin CM. 2010. Structural determinants of the substrate specificities of xylanases from different glycoside hydrolase families. Crit Rev Biotechnol 30:176–191. https://doi.org/10.3109/07388551003645599.
10. Roldán-Arjona T, Pérez-Espinosa A, Ruiz-Rubio M. 1999. Tomatinase from *Fusarium oxysporum* f. sp. *lycopersici* defines a new class of saponinases. Mol Plant Microbe Interact 12:852–861. https://doi.org/10.1094/MPMI.1999.12.10.852.
11. Nerinckx W, Broberg A, Duus JØ, Ntarima P, Parolis LA, Parolis H, Claeyssens M. 2004. Hydrolysis of *Nothogenia erinacea* xylan by xylanases from families 10 and 11. Carbohydr Res 339:1047–1060. https://doi.org/10.1016/j.carres.2004.02.017.
12. Shi P, Tian J, Yuan T, Liu X, Huang H, Bai Y, Yang P, Chen X, Wu N, Yao B. 2010. *Paenibacillus* sp. strain E18 bifunctional xylanase-glucanase with a single catalytic domain. Appl Environ Microbiol 76:3620–3624. https://doi.org/10.1128/AEM.00345-10.
13. Andrews SR, Charnock SJ, Lakey JH, Davies GJ, Claeyssens M, Nerinckx W, Underwood M, Sinnott ML, Warren RA, Gilbert HJ. 2000. Substrate specificity in glycoside hydrolase family 10. Tyrosine 87 and leucine 314 play a pivotal role in discriminating between glucose and xylose binding in the proximal active site of *Pseudomonas cellulosa* xylanase 10A. J Biol Chem 275:23027–23033. https://doi.org/10.1074/jbc.M000128200.
14. Ducros V, Charnock SJ, Derewenda U, Derewenda ZS, Dauter Z, Dupont C, Shareck F, Morosoli R, Kluepfel D, Davies GJ. 2000. Substrate specificity in glycoside hydrolase family 10. Structural and kinetic analysis of the *Streptomyces lividans* xylanase 10A. J Biol Chem 275:23020–23026. https://doi.org/10.1074/jbc.275.30.23020.
15. Notenboom V, Birsan C, Warren RA, Withers SG, Rose DR. 1998. Exploring the cellulose/xylan specificity of the beta-1,4-glycanase Cex from *Cellulomonas fimi* through crystallography and mutation. Biochemistry 37:4751–4758. https://doi.org/10.1021/bi9729211.
16. Xue X, Wang R, Tu T, Shi P, Ma R, Luo H, Yao B, Su X. 2015. The N-terminal GH10 domain of a multimodular protein from *Caldicellulosiruptor bescii* is a versatile xylanase/β-glucanase that can degrade crystalline cellulose. Appl Environ Microbiol 81:3823–3833. https://doi.org/10.1128/AEM.00432-15.
17. Li DD, Peng M, Wang N, Wang XJ, Zhang XY, Chen XL, Su HN, Zhang YZ, Shi M. 2017. *Arcticibacterium luteifluviistationis* gen. nov., sp. nov., isolated from Arctic seawater. Int J Syst Evol Microbiol 67:664–669. https://doi.org/10.1099/ijsem.0.001690.
18. Bahari L, Gilad Y, Borovok I, Kahel-Raifer H, Dassa B, Nataf Y, Shoham Y, Lamed R, Bayer EA. 2011. Glycoside hydrolases as components of putative carbohydrate biosensor proteins in *Clostridium thermocellum*. J Ind Microbiol Biotechnol 38:825–832. https://doi.org/10.1007/s10295-010-0848-9.
19. Ihsanawati, Kumasaka T, Kaneko T, Morokuma C, Yatsunami R, Sato T, Nakamura S, Tanaka N. 2005. Structural basis of the substrate subsite and the highly thermal stability of xylanase 10B from *Thermotoga maritima* MSB8. Proteins 61:999–1009. https://doi.org/10.1002/prot.20700.
20. Voget S, Steele HL, Streit WR. 2006. Characterization of a metagenome-derived halotolerant cellulase. J Biotechnol 126:26–36. https://doi.org/10.1016/j.jbiotec.2006.02.011.
21. Alvarez TM, Paiva JH, Ruiz DM, Cairo JP, Pereira IO, Paixão DA, de Almeida RF, Tonoli CC, Ruller R, Santos CR, Squina FM, Murakami MT. 2013. Structure and function of a novel cellulase 5 from sugarcane soil metagenome. PLoS One 8:e83635. https://doi.org/10.1371/journal.pone.0083635.
22. Zheng F, Ding S. 2013. Processivity and enzymatic mode of a glycoside hydrolase family 5 endoglucanase from *Volvariella volvacea*. Appl Environ Microbiol 79:989–996. https://doi.org/10.1128/AEM.02725-12.
23. Chu Y, Tu T, Penttinen L, Xue X, Wang X, Yi Z, Gong L, Rouvinen J, Luo H, Hakulinen N, Yao B, Su X. 2017. Insights into the roles of non-catalytic residues in the active site of a GH10 xylanase with activity on cellulose. J Biol Chem 292:19315–19327. https://doi.org/10.1074/jbc.M117.807768.
24. Zolotnitsky G, Cogan U, Adir N, Solomon V, Shoham G, Shoham Y. 2004. Mapping glycoside hydrolase substrate subsites by isothermal titration calorimetry. Proc Natl Acad Sci U S A 101:11275–11280. https://doi.org/10.1073/pnas.0404311101.
25. Santos CR, Hoffmam ZB, de Matos Martins VP, Zanphorlin LM, de Paula Assis LH, Honorato RV, Lopes de Oliveira PS, Ruller R, Murakami MT. 2014. Molecular mechanisms associated with xylan degradation by *Xanthomonas* plant pathogens. J Biol Chem 189:32186–32200. https://doi.org/10.1074/jbc.M114.605105.
26. Phuengmaung P, Fujiwara D, Sukhumsirichart W, Sakamoto T. 2018. Identification and characterization of the first β-1,3-D-xylosidase from a gram-positive bacterium, *Streptomyces* sp. SWU10. Enzyme Microb Technol 112:72–78. https://doi.org/10.1016/j.enzmictec.2017.11.002.
27. Martin M, Biver S, Steels S, Barbeyron T, Jam M, Portetelle D, Michel G, Vandenbol M. 2014. Identification and characterization of a halotolerant, cold-active marine endo-β-1,4-glucanase by using functional metagenomics of seaweed-associated microbiota. Appl Environ Microbiol 80:4958–4967. https://doi.org/10.1128/AEM.01194-14.
28. Miller GL, Blum R, Glennon WE, Burton AL. 1960. Measurement of carboxymethylcellulase activity. Anal Biochem 1:127–132. https://doi.org/10.1016/0003-2697(60)90004-X.
29. Nielsen H. 2017. Predicting secretory proteins with SignalP. Methods Mol Biol 1611:59–73. https://doi.org/10.1007/978-1-4939-7015-5_6.
30. Marchler-Bauer A, Bo Y, Han L, He J, Lanczycki CJ, Lu S, Chitsaz F, Derbyshire MK, Geer RC, Gonzales NR, Gwadz M, Hurwitz DI, Lu F, Marchler GH, Song JS, Thanki N, Wang Z, Yamashita RA, Zhang D, Zheng C, Geer LY, Bryant SH. 2017. CDD/SPARCLE: functional classification of proteins via subfamily domain architectures. Nucleic Acids Res 45:D200–D203. https://doi.org/10.1093/nar/gkw1129.
31. Robert X, Gouet P. 2014. Deciphering key features in protein structures with the new ENDscript server. Nucleic Acids Res 42:W320–W324. https://doi.org/10.1093/nar/gku316.
32. Kumar S, Stecher G, Tamura K. 2016. MEGA7: molecular evolutionary genetics analysis version 7.0 for bigger datasets. Mol Biol Evol 33:1870–1874. https://doi.org/10.1093/molbev/msw054.
33. Guo B, Chen XL, Sun CY, Zhou BC, Zhang YZ. 2009. Gene cloning, expression and characterization of a new cold-active and salt-tolerant endo-β-1,4-xylanase from marine *Glaciecola mesophila* KMM 241. Appl Microbiol Biotechnol 84:1107–1115. https://doi.org/10.1007/s00253-009-2056-y.
34. Winterhalter C, Liebl W. 1995. Two extremely thermostable xylanases of the hyperthermophilic bacterium *Thermotoga maritima* MSB8. Appl Environ Microbiol 61:1810–1815.